A STATISTICAL STUDY OF SPECTRAL HARDENING IN SOLAR FLARES AND RELATED SOLAR ENERGETIC PARTICLE EVENTS

2009 ApJ 707 1588

(http://iopscience.iop.org/0004-637X/707/2/1588)

The Astrophysical Journal, 707:1588–1594, 2009 December 20 doi:10.1088/0004-637X/707/2/1588

A STATISTICAL STUDY OF SPECTRAL HARDENING IN SOLAR FLARES AND RELATED SOLAR ENERGETIC PARTICLE EVENTS

James A. Grayson, Säm Krucker, and R. P. Lin[1]
Space Sciences Laboratory, University of California, Berkeley, CA 94720-7450, USA; jgrayson@berkeley.edu, krucker@ssl.berkeley.edu, rlin@ssl.berkeley.edu
Received 2009 August 28; accepted 2009 November 3; published 2009 December 7

ABSTRACT

Using hard X-ray observations from the *Reuven Ramaty High Energy Solar Spectroscopic Imager* (*RHESSI*), we investigate the reliability of spectral hardening during solar flares as an indicator of related solar energetic particle (SEP) events at Earth. All *RHESSI* data are analyzed, from 2002 February through the end of Solar Cycle 23, thereby expanding upon recent work on a smaller sample of flares. Previous investigations have found very high success when associating soft–hard–harder (SHH) spectral behavior with energetic proton events, and confirmation of this link would suggest a correlation between electron acceleration in solar flares and SEPs seen in interplanetary space. In agreement with these past findings, we find that of 37 magnetically well-connected flares (W30−W90), 12 of 18 flares with SHH behavior produced SEP events and none of 19 flares without SHH behavior produced SEPs. This demonstrates a statistically significant dependence of SHH and SEP observations, a link that is unexplained in the standard scenario of SEP acceleration at the shock front of coronal mass ejections and encourages further investigation of the mechanisms which could be responsible.

Key words: Sun: flares – Sun: particle emission – Sun: X-rays, gamma rays

Online-only material: color figures

1. INTRODUCTION

It has been observed that non-thermal hard X-ray (HXR) emission in the majority solar flares exhibits soft–hard–soft (SHS) behavior, in which the spectrum becomes harder (an increased ratio of higher to lower energies) during increased emission but then recovers to a softer spectrum when emission lessens (Parks & Winckler 1969; Grigis & Benz 2004). However, in a small fraction of events (∼15% in Kiplinger 1995), there is no spectral softening after emission peaks; instead, the spectrum becomes increasingly harder (Frost & Dennis 1971; Cliver et al. 1986). This less frequent phenomenon is referred to as progressively hardening, or soft–hard–harder (SHH), behavior. Both behaviors are manifested in the spectral index of a power-law fit to the non-thermal HXR spectrum, with a lower spectral index corresponding to a harder spectrum.

These different characteristics of the HXR spectrum provide information regarding electron kinematics during flares, as the non-thermal HXR continuum of interest is a signature of bremsstrahlung emission radiated by decelerating electrons. Spectral softening and hardening behavior therefore gives possible insight into the electron acceleration mechanisms of flares (e.g., Grigis & Benz 2006). Additional support of this link between non-thermal HXR spectra and flare acceleration processes is given by Kiplinger (1995), which found an extremely high, 96% success rate when relating solar energetic particle (SEP) events observed at Earth to SHH behavior in the associated flares.

The primary goal of this paper is to further investigate Kiplinger's correlation of SHH behavior in solar flares and SEP events at Earth. Similar to Saldanha et al. (2008), SHH behavior is determined using high-resolution HXR observations from the *Reuven Ramaty High Energy Solar Spectroscopic Imager* (*RHESSI*; Lin et al. 2002) and we predominantly judge SEP occurrences based on in situ proton observations by the *Geostationary Operational Environmental Satellites* (*GOES*) (other data sources are covered in Section 2.3). However, while the Saldanha study confirmed Kiplinger's results by analyzing five large flares (*GOES* X-class) from the 2005 January solar storm, the current study considers the entire *RHESSI* catalog of M- and X-class flares (through the end of Solar Cycle 23) in a statistical manner more akin to the original Kiplinger treatment.

Since they are a major source of motivation and comparison, it is helpful to summarize the Kiplinger (1995) results before continuing. Using 10 years of HXR data from the Hard X-ray Burst Spectrometer (HXRBS) aboard the *Solar Maximum Mission* (Orwig et al. 1980), the study considered all 731 flares with peak count rates >800 counts s^{-1} (Dennis et al. 1991, ∼30–500 keV), full observational coverage (beginning and ending with at most ∼10% of peak count rate), and clear SEP events/non-events. SEP occurrences were based on the published NOAA Solar Proton Events Affecting the Earth Environment list,[2] which considers a proton event to be >10 particles cm^{-2} s^{-1} sr^{-1} at >10 MeV for >15 minutes, as determined by *GOES*. It is worth mentioning that only 345 flares in the Kiplinger study were actually inspected for SHH and SEP events, the remaining 386 results being extrapolated from this subset.

Based on preliminary results, two criteria were employed in addition to SHH behavior for predicting an SEP event: no SEP prediction if SHH behavior is limited to HXR flux peaks lasting <70 s FWHM, and no SEP prediction if the event has both a peak flux below *GOES* X1 and a solar location east of E40 (this second condition was misworded in Saldanha et al. 2008). In total, the Kiplinger (1995) study found that 96% (22/23) of SEP-producing flares were predicted by SHH and the two prediction criteria. Or, viewing the results in another way, 73% (22/30) of SEP-*predicting* flares actually gave rise to an SEP; it is this ratio that we consider in the current study.

[1] Also at Department of Physics, University of California, Berkeley, CA 94720-7300, USA.

[2] Available online: www.swpc.noaa.gov/ftpdir/indices/SPE.txt

2. DATA AND ANALYSIS

2.1. Flare Selection

Using *RHESSI* observations from 2002 February 12 (the first data after launch) through the end of Solar Cycle 23, we selected all *GOES* X- and M-class flares to create an initial data set of 661 events. The minimum M-class condition was chosen to obtain a workable sample size while maintaining comparable breadth to the Kiplinger (1995) data. Three additional selection criteria were then imposed on the data set:

(1) *Flares were limited to solar locations within W30 and W90 longitude*, to ensure that any associated SEP events were likely to be observed at Earth. This region of the Sun is generally considered "well connected" to Earth by interplanetary magnetic field lines. Using the Parker spiral model and typical solar wind speeds, it has been shown that average spiral footpoint locations are within 30° of W60 (e.g., Krucker et al. 1999). It is also possible that larger flares are more capable of propagating particles from less-connected solar locations (Belov et al. 2005); Kiplinger (1995) initially observed this phenomena (only flares >X5 with SHH behavior had associated SEP events when east of E35), and consequently excluded events which were both <X1 and east of E40 in his final data set. We elected, however, to confine our current study to well-connected locations in order to avoid using class-dependent selection criteria and the related biases. Of course, the drawback of this decision was the quick downsizing of our data set: only 183 of the 661 events lie within W30 and W90.

Flare locations were determined using *RHESSI* imaging capabilities (see Hurford et al. 2002). In a few cases, the satellite's aspect system failed to provide sufficient satellite–Sun relative position data, and flare coordinates could not be determined. Events with undetermined locations were removed from the data set; however, only two events which satisfied the following two selection criteria had to be excluded for this reason.

(2) *Flares must have had at least partial observational coverage*. *RHESSI* orbits Earth every ∼96 minutes with ∼36 minutes of night and occasional downtime due to the South Atlantic Anomaly; inevitably, a significant fraction of solar activity is not observed by the satellite. In an attempt to salvage some of this data, we included flare events that were only partially observed, in addition to those with full coverage. Observations were considered only "partial" if pre- and post-peak coverage did not diminish to ∼10% of *GOES* peak soft X-ray (SXR) flux, there were any missed sub-peaks in *GOES* SXR flux, or if the event had an unobserved, extremely slow SXR post-peak decay (which is often where we found progressive HXR hardening behavior, see Figure 1, top). This method of judging the observational coverage seemed more appropriate than an arbitrary flux cutoff alone, given the huge variation in flare characteristics. Of the 661 total events, 163 had full and 362 had partial coverage by *RHESSI*.

There are two important considerations when using partially observed events. First, care must be taken with these events in our final statistics. Specifically, when calculating what percentage of flares *without* SHH behavior gave rise to an SEP event, only flares with full coverage can be included; partially observed events could have exhibited SHH behavior during *RHESSI* downtime. Second, by not setting rigid pre- and post-peak cutoff fluxes in determining full or partial coverage, we admittedly introduce some subjectivity (but show it to be negligible in Section 3). This is not the only area in which some qualitative analysis appeared to be the best option, and such limitations in SHH/SEP studies are further discussed in Section 4.

(3) *Flares must have clearly exhibited non-thermal hard X-rays above background levels*. The *RHESSI* spacecraft is a lightweight, NASA Small Explorer mission, with less than an eighth of the mass of the *Solar Maximum Mission* spacecraft that carried HXRBS (Chipman 1981; Lin et al. 2002). Its low mass is partially due to a lack of shielding around its detectors, resulting in relatively higher background radiation levels. *RHESSI* spectrograms (e.g., Krucker & Lin 2002) were individually inspected to ensure that there was enough non-thermal HXR emission above background levels to be analyzed by a power-law fit, since many of the smaller events exhibited mostly lower-energy thermal emission. A quantitative check to assure that small fluctuations in background levels would not influence our results is described in the next section. In total, we found that 123 of 163 fully observed events, and 173 of 362 partially observed events, showed sufficient non-thermal emission above background levels.

After applying all three selection criteria, we were left with 84 flares which could then be further analyzed for SHH behavior and SEP event correlation. Of these 84 flares, 32 had full and 52 had partial observational coverage by *RHESSI*.

2.2. Spectral Evolution

Each flare's spectral evolution was then investigated to identify those with progressive non-thermal HXR hardening, or SHH, behavior. For this purpose, we used *RHESSI* front-segment count rates (Smith et al. 2002), binned into 4 s time steps and covering ∼3–200 keV. Since we were only interested in the relative behavior of the spectra through time, using count rate data without full calibration greatly simplified the analysis process. This did not introduce any significant bias, as the *RHESSI* response is fairly linear in the relevant non-thermal HXR energy range of ∼30–100 keV (Smith et al. 2002).

The only reduction performed before fitting was nighttime background subtraction; not correcting for count pile-up, decimation, or attenuator effects did not affect the results. *RHESSI*'s count pile-up, the recording of simultaneous photons as a single higher-energy photon, primarily affects the lowest energies in the 30–100 keV range considered. Therefore, while pile-up may soften the spectrum during periods of very high emission, it cannot create the asymmetrical progressive hardening characteristic of SHH behavior. Decimation refers to the deletion of a fraction of counts below a certain energy in order to save spacecraft memory. When present, this energy cutoff was below 35 keV and easily avoided when selecting each flare's power-law energy range. Lastly, *RHESSI* often uses aluminum attenuators to prevent saturation of its detectors, resulting in a decrease of lower-energy count rates. On the spectrograms, these regions of varying detector sensitivity were clearly distinguishable from solar activity and did not influence the inspection for SHH behavior.

The non-thermal HXR energy range was individually determined for each flare before fitting to ensure that there was enough signal above background to be analyzed. The lower bound of this energy range was typically 30–40 keV, while the upper bound could be ∼50 keV for smaller events and as high as 100 keV for events exhibiting considerable HXRs. There was concern that the necessarily harder background emission could produce false SHH observations, especially at the highest energies considered, where count rates are lower. To be sure that this was not a problem, the time variations in the background rates

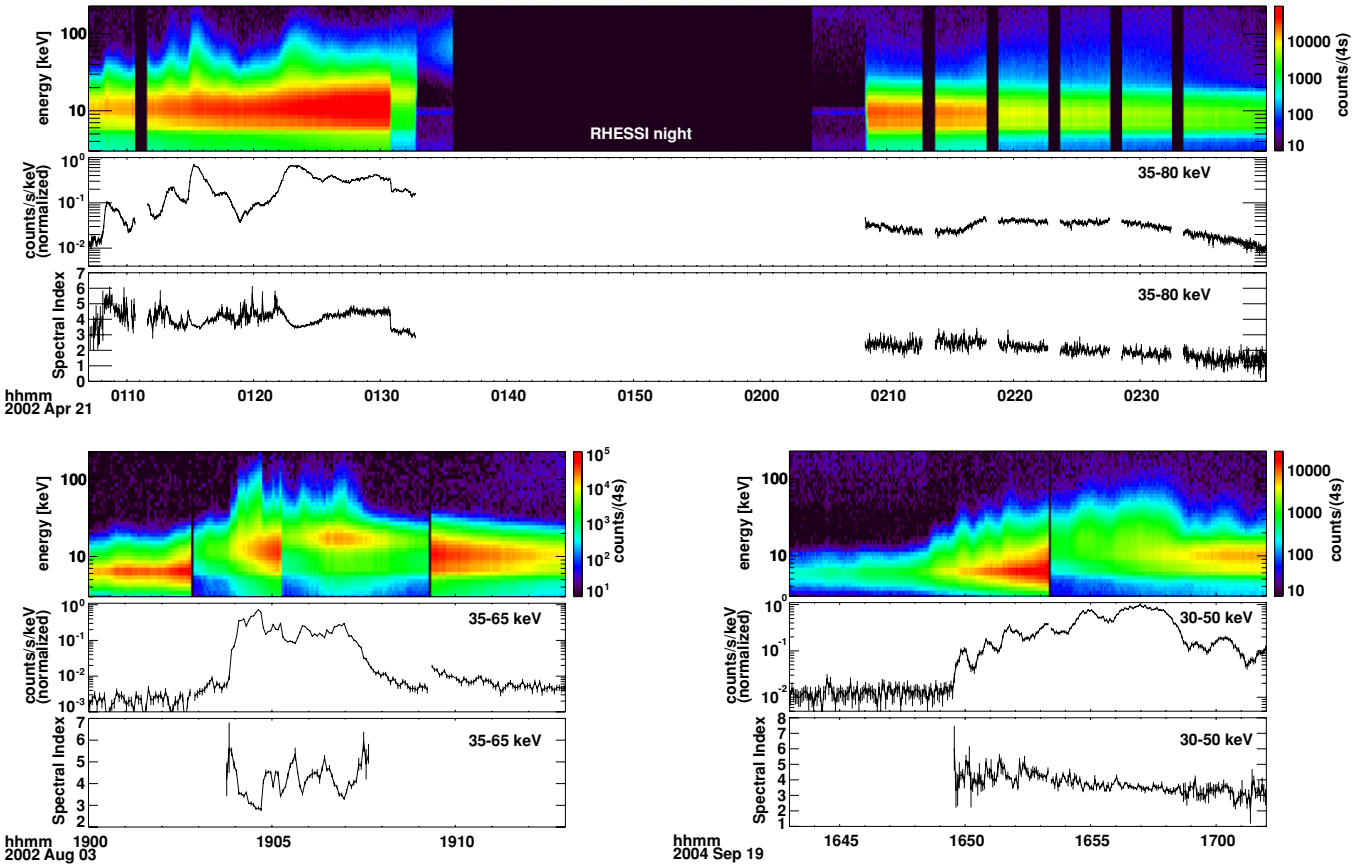

Figure 1. Top: *RHESSI* spectrogram, HXR light curve, and corresponding spectral indices of the 2002 April 21 (X1.5) flare. SHH behavior, seen as a progressively decreasing spectral index, occurs around half an hour after the unobserved SXR peak at 01:51. This late appearance of SHH behavior emphasizes the importance of the "partial" vs. "full" observational coverage distinction. Data have been removed during rapid *RHESSI* attenuator activity for easier viewing. Bottom left: the 2002 August 3 19:07 (X1.0) flare, a clear example of SHS spectral behavior in which the spectral index appears as the inverse of the HXR light curve. Bottom right: the 2004 September 19 17:12 (M1.9) flare exhibited strong SHH behavior, seen as a continuously decreasing spectral index. In both bottom examples, the spectral index is only plotted during times of non-thermal HXR emission above background, and data have been removed during *RHESSI* attenuator movement for clearer viewing.

(A color version of this figure is available in the online journal.)

were visually inspected for each event. Additionally, signal-to-background ratios were calculated for flares which exhibited SHH behavior (see Table 1). Ratios considered the counting rates at the onset of SHH, and just before the *GOES* flare start time or during *RHESSI* night, whichever was closer to the SHH behavior, each measurement lasting for 1 minute. Both counting rates were calculated in the top 10 keV of the energy range used for fitting the power law. The average signal-to-background ratio for the 18 flares with SHH was 15.6, assuring that even at the highest energies there was enough signal to not be influenced by slight variations in background levels.

Within this non-thermal HXR energy range, we assumed a single power-law distribution,

$$I \propto E^{-\gamma}, \tag{1}$$

in which the counts I are a function of the energy E and γ is the spectral index. Linear fits of the spectra to this power-law form were performed using the standard IDL routine REGRESS.

Flares were visually inspected for SHH behavior by comparing the spectral index (γ) time-progression to a light curve of counts integrated across the non-thermal HXR energy range (Figure 1). A harder spectrum has a lower γ value, and therefore appears flatter. SHH behavior is defined here as a continuously decreasing γ through non-thermal HXR emission peaks, with no recovery to higher γ values when emission lessens. In most events, we only observed the more typical soft–hard–soft (SHS) behavior, for which the γ time-progression appears as a "mirror image" of the light curve (Figure 1, bottom, shows characteristic examples of both SHH and SHS behavior). Also, after proving too difficult to confidently judge, 18 flares were excluded from further study. Often, these indeterminable events had very little non-thermal HXR emission above background levels, the HXR emissions lasted only a few minutes, or there was contamination by magnetospheric counts.

2.3. Energetic Particles

The final step of analysis was to look at energetic particle data during times immediately following the flares. As in previous studies (Kiplinger 1995; Saldanha et al. 2008), SEP events were primarily determined by in situ proton flux measurements. In difficult cases, electron flux measurements were also used for corroboration (Figure 2). We consulted *GOES* >10 MeV proton data, and both ~0.1–7 MeV proton and ~30–500 keV electron data from the foil and open semiconductor detectors of the 3-D Plasma and Energetic Particle experiment aboard the *WIND* spacecraft (Lin et al. 1995). In addition to the clear advantage of considering data from two different spacecraft locations, the less energetic particle data from *WIND* provided correspondingly higher particle fluxes that greatly aided SEP detection. No minimum particle flux level was required to be considered an

Table 1
Flares Included in Final Results

GOES SXR Peak Time	*GOES* Class	*GOES* Duration (minutes)[a]	*RHESSI* Location	*RHESSI* Observational Coverage	SHH Signal to Background Ratio	SHH Behavior	SEP Event	NOAA SEP Event	LASCO CME Velocity (km s^{-1})
2002 Feb 25 02:57	M1.0	13	S19,W68	Full	...	No	No	No	...
2002 Apr 15 00:14	M3.7	51	N20,W61	Full	...	No	No	No	...
2002 Apr 17 08:24	M2.6	131	S12,W36	Partial	8.4	Yes	Yes	Yes	1240
2002 Apr 21 01:51	X1.5	115	S13,W89	Partial	4.8	Yes	Yes	Yes	2393
2002 Apr 24 21:56	M1.7	15	N10,W50	Full	...	No	No	?	576
2002 Jul 3 02:13	X1.5	8	S20,W50	Full	12.8	Yes	No	No	265
2002 Aug 2 10:53	M1.0	10	S15,W64	Full	...	No	No	No	...
2002 Aug 3 19:07	X1.0	12	S16,W87	Full	...	No	No	No	1150
2002 Aug 21 01:41	M1.4	10	S10,W48	Full	20.8	Yes	No	No	400
2002 Aug 28 21:45	M1.1	11	S27,W85	Full	...	No	No	No	...
2002 Oct 31 16:52	X1.2	8	N29,W87	Full	...	No	No	No	...
2002 Dec 22 02:52	M1.1	58	N22,W45	Partial	14.8	Yes	No	No	1071
2003 Mar 18 12:08	X1.5	29	S14,W47	Partial	10.2	Yes	Yes	No	1601
2003 Apr 24 12:53	M3.3	18	N19,W36	Partial	17.3	Yes	Yes	No	609
2003 Apr 26 00:58	M2.1	9	N19,W65	Full	...	No	No	No	690
2003 Apr 26 03:06	M2.1	11	N18,W66	Full	...	No	No	No	289
2003 Apr 26 23:40	M2.5	5	N18,W79	Full	...	No	No	No	386
2003 Apr 27 15:32	M1.7	8	N20,W88	Full	...	No	No	No	513
2003 May 29 01:05	X1.2	21	S07,W32	Full	8.5	Yes	No	?	1237
2003 Jun 9 11:28	M4.7	12	N14,W31	Full	...	No	No	No	749
2003 Jun 10 11:12	M5.1	20	N13,W44	Full	...	No	No	No	762
2003 Jun 13 04:37	M1.7	12	N10,W89	Full	...	No	No	No	...
2003 Nov 1 22:38	M3.2	23	S13,W62	Partial	9.7	Yes	No	No	899
2003 Nov 2 17:25[b]	X8.3	36	S18,W58	Partial	17.6	Yes	Yes	Yes	2598
2004 Apr 15 16:44	M1.2	11	S15,W39	Full	...	No	No	No	276
2004 Aug 17 05:06	M1.1	15	S12,W70	Full	...	No	No	No	...
2004 Sep 19 17:12	M1.9	53	N03,W58	Partial	9.8	Yes	Yes	Yes	unknown[d]
2004 Nov 10 02:13[b]	X2.5	21	N08,W47	Full	8.3	Yes	Yes	?	3387
2005 Jan 19 08:22[b]	X1.3	37	N15,W51	Full	26.5	Yes	No[c]	?	2020
2005 Jan 19 10:24	M2.7	10	N17,W46	Full	...	No	No	No	823
2005 Jan 20 07:01[b]	X7.1	50	N13,W64	Partial	22.2	Yes	Yes	?	882
2005 Jan 21 10:16	M1.7	9	N17,W74	Full	...	No	No	?	273
2005 May 11 19:38	M1.1	33	S11,W52	Partial	30.8	Yes	Yes	No	550
2005 Jul 13 14:49	M5.0	97	N10,W89	Partial	36.0	Yes	Yes	Yes	1423
2005 Aug 22 01:33	M2.6	94	S10,W54	Partial	16.8	Yes	Yes	No	1194
2006 Apr 6 05:33	M1.4	14	S08,W54	Full	...	No	No	No	173
2006 Dec 14 22:15	X1.5	79	S06,W45	Partial	5.2	Yes	Yes	?	1042
Flares only included when applying Kiplinger's prediction algorithm									
2002 Feb 20 09:59	M4.3	18	N20,W87	Full	...	No	?	No	623

Notes. Question marks indicate that it was unclear whether or not an SEP event occurred. Ellipses in the last column indicate that there was no associated CME.

[a] *GOES* event duration is defined by NOAA to begin in the first minute of monotonic increase in SXR flux, and to end when SXR flux decays to halfway between the peak flux and the pre-flare background level.

[b] The 2003 November 2 17:25, 2004 November 10 02:13, 2005 January 19 08:22, and 2005 January 20 07:01 flares are also *RHESSI* γ-ray flares as listed in Shih et al. (2009).

[c] The 2005 January 19 08:22 flare was found to produce an SEP event in Saldanha et al. (2008), using data from the Ultra Low Energy Isotope Spectrometer aboard the *Advanced Composition Explorer* (Mason et al. 1998). Since this particle event was not evident in the *GOES* or *WIND* data used presently, we consider there to be no SEP for consistency.

[d] While it is clear that a CME occurred, velocity values are not available for the 2004 September 19 17:12 flare due to a gap in the LASCO CME data.

SEP event; we are interested in investigating which flares give rise to interplanetary accelerated particles, regardless if that flux is particularly intense at Earth. The typical background flux level above which we could detect proton increases was $\sim$0.1 particles cm^{-2} s^{-1} sr^{-1} at $>$10 MeV.

When occurring after periods of no activity above background levels, SEP events were easily detected. However, especially during periods of high flaring activity, SEP events often overlapped each other and made it difficult to retrace individual particle events to corresponding flares (Figure 2 is an example). SEP events were therefore judged by several criteria in conjunction with the *GOES* and *WIND* data, in order to maintain consistency among these difficult cases. (1) An SEP occurred if there was a clearly identifiable proton rise in either data set, or if there was a small, less obvious proton increase with a clearly related electron rise. (2) No SEP occurred if there was an electron rise but no identifiable proton increase, or if the event overlapped a smoothly decaying earlier proton increase but did not have a corresponding electron peak. (3) An SEP event was left as indeterminable if the event overlapped a smoothly decaying

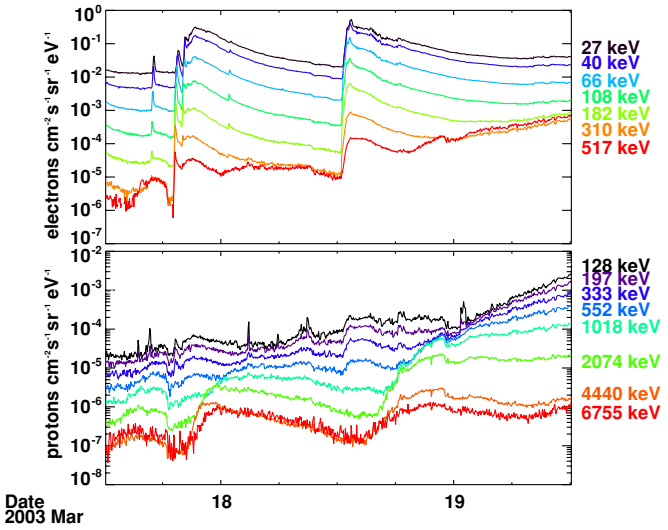

Figure 2. *WIND*/3DP energetic particle data covering 24 hr before and after the 2003 March 18 12:08 (X1.5) flare. While there is a high amount of proton activity (bottom panel), the obvious electron flux peak occurring just after 12:00 on March 18 (top panel) helps to illuminate a gradual rise in proton flux that originates from this flare. Also visible in this example is cross-contamination of species in each detector: the highest energy electron curve (517 keV) displays a gradual rise after 18:00 on March 18 because high-energy protons were able to penetrate the electron detector's foil shield; similarly, the electron peak is visible in the lower-energy proton curves because high-energy electrons traveled though the proton detector's magnetic shield.

(A color version of this figure is available in the online journal.)

earlier proton increase and had an identifiable electron rise, or if the event overlapped the erratic decay of an earlier proton increase. Six flares, in addition to the 18 which were removed due to indeterminable spectral behavior, had to be excluded from the data as indeterminable SEP cases, resulting in 60 flares which were completely analyzed.

3. RESULTS

Of these 60 remaining flares, 37 could be included in the final results (Table 1 lists these events). We were required to ignore the 23 events which had only partial observational coverage and no observed SHH, as SHH behavior could have occurred out of *RHESSI*'s view. Ultimately, two-thirds of the 18 flares with SHH gave rise to SEPs, and maybe more revealing, *none* of the 19 flares without SHH behavior had an associated SEP event. Organizing these 37 events into a 2 × 2 contingency table (Table 2), the chi-square value when assuming the null hypothesis of no SEP/SHH correlation could be calculated using

$$\chi^2 = \frac{n(ad - bc)^2}{(a+c)(b+d)(c+d)(a+b)}, \quad (2)$$

where n is the total sample size (37 flares) and a, b, c, and d each refer to one cell of the contingency table (Daniel 1990). We found $\chi^2 = 18.7$, corresponding to a rejection of the null hypothesis at greater than 99.5% confidence. This clearly establishes a statistically significant correlation between SEP and SHH occurrence in flares. These results, along with those of Kiplinger (1995) and Saldanha et al. (2008), are shown in Figure 3.

For direct comparison to Kiplinger (1995), the final results were also recalculated using the NOAA SEP list along with the two additional selection criteria. Table 1 includes the NOAA SEP data, although several are left as questionable

Table 2
2 × 2 Contingency Table of Final Results

Spectral Behavior	SEP Event	No SEP Event
SHH:	$a = 12$	$b = 6$
No SHH:	$c = 0$	$d = 19$

Note. a, b, c, and d refer to Equation (2).

and excluded from calculation, since the NOAA criteria do not account for flares that occur during above-threshold proton flux from an earlier event. Three flares (2002 July 3, 2002 August 21, and 2002 December 22) were also excluded because SHH was limited to HXR peaks lasting <70 s FWHM. One additional flare, which was not used in our original results due to indeterminable SEP occurrence, could be included using the NOAA list (see the bottom of Table 1). We found that 5 of 10 SEP-predicting flares gave rise to SEP's, while none of 18 non-SEP-predicting flares produced SEP events, giving a similar correlation to the original result. We found $\chi^2 = 11$, again indicating a confidence level of greater than 99.5%.

As a quick check, we addressed the possible bias introduced when judging "full" versus "partial" observational coverage of flares by *RHESSI*, this being one of the most prominent factors that differentiated this study from Kiplinger (1995). The concern stems from the fact that "partial" events are discarded if they do not exhibit SHH behavior, since the progressive hardening could have been unobserved by the spacecraft. Therefore, partially covered events with SEPs but no SHH behavior were unable to contradict the SEP/SHH correlation. In order to test this influence on the final statistics, these excluded events were temporarily considered to have full coverage if the *RHESSI* observations spanned the listed *GOES* flare duration (to within a minute). These durations were generally much shorter than those implied by the study's selection criteria. This adjustment led to the inclusion of nine additional flares with no SHH behavior observed, and eight of these events did not produce SEPs, thereby supporting the original results ($\chi^2 = 21.5$, again giving >99.5% confidence). Only one flare (2006 July 06 08:36, M2.5) resulted in SEPs, but it exhibited the unobserved, long (>30 minutes) SXR decay that we wanted to avoid by using the selection criteria.

Another brief sub-study considered the peak flux, location, and duration of the six flares that showed SHH behavior but were "missing" SEP events, in the hope of understanding why these specific flares did not follow the SEP/SHH correlation. One possibility was, for example, that these flares occurred at the edges of the W30−W90 longitudinal range, therefore suggesting that they were simply less well connected to Earth than the other events. However, looking at the data, we find no such obvious correlation in location, or in *GOES* class and duration (Figure 4). The six SEP-lacking flares do seem confined to lower peak flux and durations (<X2, <60 minutes), but this region in parameter space is not exclusive, also containing four SEP-producing flares. Believing the SEP/SHH correlation to be true, the best explanation for the missing SEP events might be the complex and dynamic interplanetary magnetic fields. The Parker spiral model, used to determine the "well-connected" solar region, is of course an oversimplification, but it is beyond the scope of this study to attempt to reconstruct the conditions of the solar wind for individual flares.

Lastly, the relationship of progressive hardening and energetic particle events to coronal mass ejections (CMEs) was

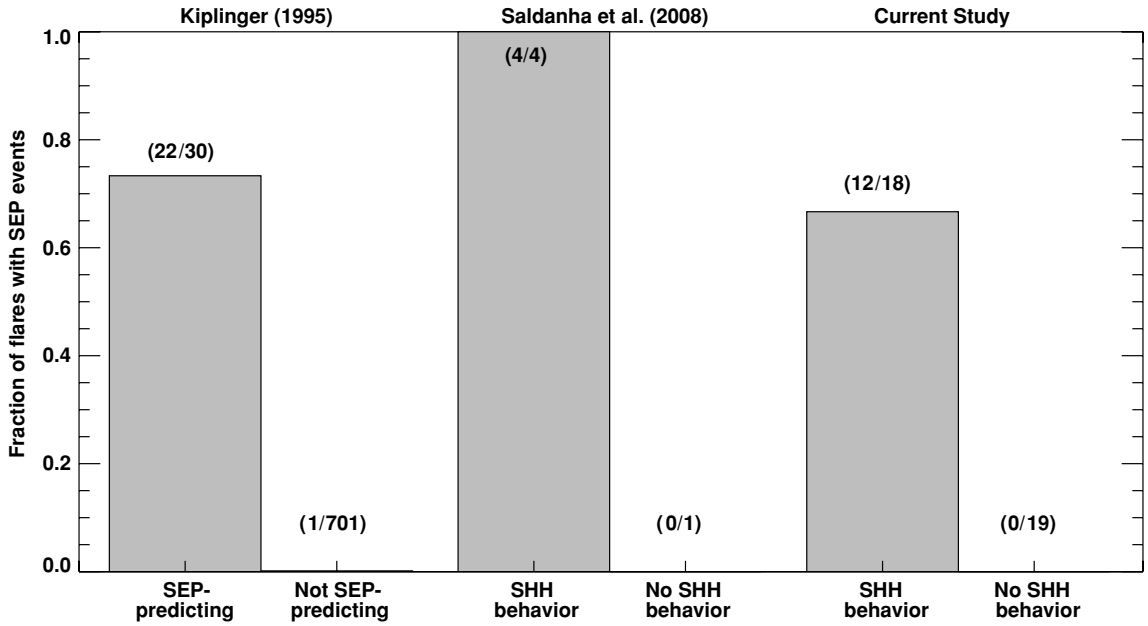

Figure 3. Overview of results from the current and two previous studies. The fraction of flares which resulted in SEP events is shown, grouped by study and whether or not the flares displayed SHH behavior. The Kiplinger (1995) categories are identified as SEP- and non-SEP-predicting to signify the two prediction criteria used in addition to SHH behavior. From left to right, $\chi^2 = 506$, 5.0, and 18.7, corresponding to a rejection of the null hypothesis (no SHH/SEP correlation) at greater than 99.5% confidence, not including the insufficient sample size of Saldanha et al. (2008).

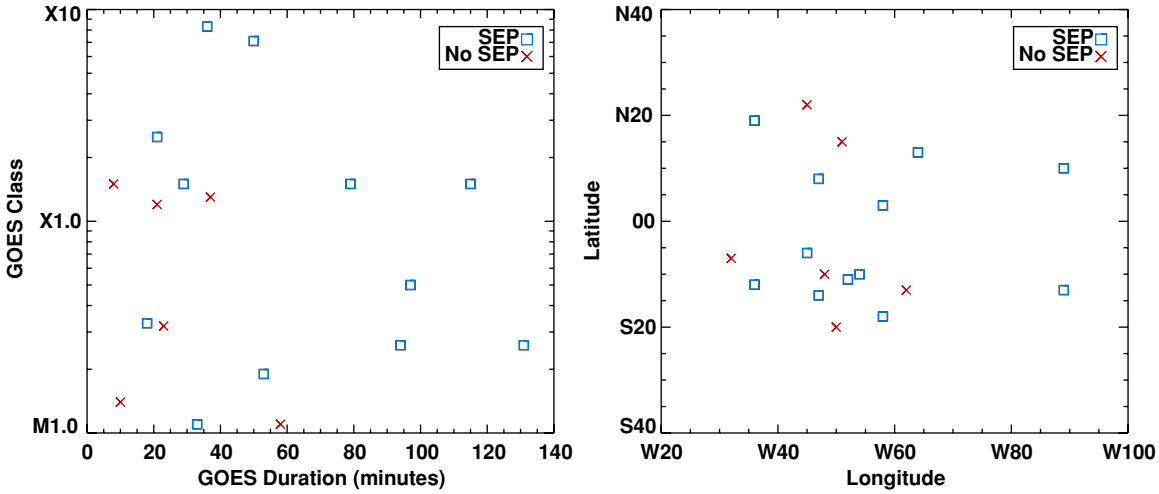

Figure 4. All 18 flares that exhibited SHH, plotted as functions of *GOES* class and duration, and *RHESSI* solar location. No distinct pattern regarding SEP production is apparent.

(A color version of this figure is available in the online journal.)

investigated. For all 37 flares used in our final results, we gathered apparent CME velocity (linear-fit) data from the *SOHO* LASCO CME catalog[3] (see Table 1). As is shown in Table 3, the majority of flares were associated with CMEs, and all seven flares that did not have an associated CME also lacked SHH behavior (and therefore did not produce SEPs). The fact that all progressively hardening flares were linked to a CME, regardless of SEP occurrence, further distinguishes the SHH population from other flares. This difference is again apparent when considering the average CME velocities: CMEs related to SHH flares had an average speed of 1342 km s^{-1}, much greater than the average 555 km s^{-1} of those related to non-SHH flares. For comparison, Yashiro et al. (2004) reported LASCO catalog averages of 428 km s^{-1} for normal CMEs (angular width between 20° and 120°) and 957 km s^{-1} for halo CMEs. Average CME velocities were also greater for flares with both progressive hardening and particle events than for those with only progressive hardening (1538 km s^{-1} versus 982 km s^{-1}; see Table 3), and may be related to an explanation of the "missing" SEP events.

4. DISCUSSION

The study has found a statistically significant correlation between SHH spectral behavior in solar flares and the production of SEP events at Earth, in agreement with the previous work of Kiplinger (1995) and Saldanha et al. (2008). However, our sample size is over seven times larger than that of the latter, and

[3] This CME catalog is generated and maintained at the CDAW Data Center by NASA and The Catholic University of America in cooperation with the Naval Research Laboratory. *SOHO* is a project of international cooperation between ESA and NASA. Available online: cdaw.gsfc.nasa.gov/CME_list/

Table 3
CME Statistics of Final Results

CME Statistic	SHH and SEP	SHH Only	No SHH and No SEP
CME:	12	6	12
No CME:	0	0	7
Average Velocity (km s^{-1}):	1538	982	555

there are important differences between ours and Kiplinger's treatment of the problem. Most importantly, we attempted to avoid any unnecessary selection criteria and the associated biases. The two additional criteria of Kiplinger (1995)—that SHH must be exhibited on emission peaks >70 s and that flares east of E40 must be >X1—clearly created a filter for better results, but this was justified by presenting the study as a practical prediction algorithm for major proton events that are dangerous to space missions (thereby also validating the high threshold of the NOAA proton event list). In contrast, the goal of this paper is to provoke further investigations into the actual mechanisms that could relate SHH and SEP occurrences, with less concern for prediction methods. Another significant difference in the two studies is evidenced by the separation in sample sizes: as discussed previously, our selection for full observational coverage of flares was rather strict, largely owing to the use of *GOES* SXR light curves to determine flare durations rather than the much shorter HXR emission phases.

In the end, the agreement of the three studies' results, despite differing data and methods, seems to further ratify the SEP/SHH link. This agreement of results may be especially meaningful considering the inherently subjective nature of all SHH investigations. Unfortunately, there is currently no way to automate the detection of spectral hardening objectively and robustly, and these studies are therefore unable to avoid some judgment calls. Until a better understanding of the mechanisms that cause SHH behavior is available, it is difficult to know which flare selection methods and judgment criteria for SHH are reasonable and which are detrimental.

Finally, while the primary focus of this paper was to evaluate the statistical nature of the SHH and SEP relationship, we want to mention some possible ideas about the processes involved in progressively hardening behavior. Grigis & Benz (2008) studied five large flares observed by *RHESSI* that showed initial SHS behavior and a gradual SHH hardening phase as emission lessened. By tracking the positions of HXR emission sources during the transition from SHS to SHH phases, it was found that the source positions did not change abruptly or in any consistent trend. They concluded that the acceleration mechanisms during both SHS and SHH are likely different behaviors of the same process, which undergoes a gradual transition. Longer trapping times in the same accelerator before precipitation to footpoints is one possibility that agrees with this finding, and some conditions for this process are discussed in Saldanha et al. (2008).

In contrast, during one X-class flare observed by *Yohkoh*/HXT, Qiu et al. (2004) observed differences in the footpoint motions, locations, and emission characteristics during the SHS and SHH phases. A separation motion of footpoints and an energy-dependent time lag of HXR emission during the hardening period suggested that a separate mechanism was active, such as second-step acceleration and subsequent precipitation in a "collapsing-trap" model. Tomczak (2008) also found evidence of distinct SHS and SHH acceleration mechanisms, although while studying coronal HXR sources rather than thick-target footpoint emission: in *Yohkoh*/HXT observations of three partially occulted flares, the onset of progressively hardening behavior was concurrent with the appearance of a distinct coronal source. Coronal γ-ray bremsstrahlung sources related to SHH behavior are also reported by Krucker et al. (2008). In addition, CME information may provide insight into progressively hardening flares; our study found that all SHH events had corresponding CMEs, and that average CME speeds for SHH flares were much greater than those of non-SHH flares (1342 km s^{-1} versus 555 km s^{-1}).

These numerous and competing views outline the need to further study and understand the production of SHH behavior, as this will be an essential first step to obtaining a complete picture of the SHH, SEP, and CME shock front relationship.

We thank the referee for helping to improve the scope of our investigation and discussion. This work was supported through NASA contract NAS 5-98033 for *RHESSI* and grant NNG 05GH18G for *WIND*.

Facilities: RHESSI

REFERENCES

Belov, A., Garcia, H., Kurt, V., Mavromichalaki, H., & Gerontidou, M. 2005, Sol. Phys., 229, 135
Chipman, E. G. 1981, ApJ, 244, L113
Cliver, E. W., Dennis, B. R., Kiplinger, A. L., Kane, S. R., Neidig, D. F., Sheeley, N. R., Jr., & Koomen, M. J. 1986, ApJ, 305, 920
Daniel, W. W. 1990, Applied Nonparametric Statistics (2nd ed.; Boston, MA: PWS-KENT)
Dennis, B. R., Orwig, L. E., Kennard, G. S., Labow, G. J., Schwartz, R. A., Shaver, A. R., & Tolbert, A. K. 1991, NASA STI/Technical Memorandum 4332
Frost, K. J., & Dennis, B. R. 1971, ApJ, 165, 655
Grigis, P. C., & Benz, A. O. 2004, A&A, 426, 1093
Grigis, P. C., & Benz, A. O. 2006, A&A, 458, 641
Grigis, P. C., & Benz, A. O. 2008, ApJ, 683, 1180
Hurford, G. J., et al. 2002, Sol. Phys., 210, 61
Kiplinger, A. L. 1995, ApJ, 453, 973
Krucker, S., Larson, D. E., Lin, R. P., & Thompson, B. J. 1999, ApJ, 519, 864
Krucker, S., & Lin, R. P. 2002, Sol. Phys., 210, 229
Krucker, S., Hurford, G. J., MacKinnon, A. L., Shih, A. Y., & Lin, R. P. 2008, ApJ, 678, L63
Lin, R. P., et al. 1995, Space Sci. Rev., 71, 125
Lin, R. P., et al. 2002, Sol. Phys., 210, 3
Mason, G. M., et al. 1998, Space Sci. Rev., 86, 409
Orwig, L. E., Frost, K. J., & Dennis, B. R. 1980, Sol. Phys., 65, 25
Parks, G. K., & Winckler, J. R. 1969, ApJ, 155, L117
Qiu, J., Lee, J., & Gary, D. E. 2004, ApJ, 603, 335
Saldanha, R., Krucker, S., & Lin, R. P. 2008, ApJ, 673, 1169
Shih, A. Y., Lin, R. P., & Smith, D. M. 2009, ApJ, 698, L152
Smith, D. M., et al. 2002, Sol. Phys., 210, 33
Tomczak, M. 2008, Cent. Eur. Astrophys. Bull., 32, 59
Yashiro, S., Gopalswamy, N., Michalek, G., St. Cyr, O. C., Plunkett, S. P., Rich, N. B., & Howard, R. A. 2004, J. Geophys. Res. (Space Phys.), 109, 7105